INTERNATIONAL JOURNAL OF PRECISION ENGINEERING AND MANUFACTURING Vol. 19, No. 4, pp. 463-471 APRIL 2018 / 463
REGULAR PAPER
DOI: 10.1007/s12541-018-0056-5
ISSN 2234-7593 (Print) / 2005-4602 (Online)

An Investigation on the Motion Error of Machine Tools' Hexapod Table

Mohammad Reza Chalak Qazani[1,#], Siamak Pedrammehr[2], and Mohammad Javad Nategh[1]

1 Faculty of Technology & Engineering, Department of Mechanical Engineering, Tarbiat Modares University, Tehran, Iran
2 Institute for Intelligent Systems Research and Innovation (IISRI), Deakin University, Waurn Ponds Campus, Victoria 3217, Australia
Corresponding Author / E-mail: m.r.chalakqazani@gmail.com, TEL: +989364197107
ORCID: 0000-0003-1839-029X

KEYWORDS: Hexapod, Circular interpolation, Improved tustin algorithm, Nonlinear error, Image processing

Accuracy is greatly affected by the nonlinear motion of hexapods. This need is more apparent when these mechanisms are employed in machining industry where precision and surface qualities are of critical importance. In this paper, a comprehensive algorithm for tool path programming of the hexapod table is developed. This algorithm is developed based on a circular motion in C#.Net and has the capability of investigating nonlinear motion error to keep it in a controlled range as well. Improved Tustin algorithm is used for interpolating circular path. The effects of different parameters on the nonlinear error of machine tools' hexapod table during circular interpolation are also investigated in this study. In the circular motion, the optimal radius which provides access to maximum feed rate with least error is obtained by solving Tustin and nonlinear error equations. The results obtained by the theoretical method are further verified through image processing experimental tests. It is found that the results of theoretical analysis and experimental test are in good consistency.

Manuscript received: March 8, 2017 / Revised: October 1, 2017 / Accepted: December 21, 2017

1. Introduction

The general demand for the design of the machine tool for high-speed machining is in the high acceleration capability of the machine axes while simultaneously meeting the high demands on accuracy.[1] Currently, most of the machine tools are designed on basis of using simple open kinematic chain. Such multi-axis mechanisms suffer from the disadvantage that each axis must either move or carry other axes that are placed further along the kinematic chain. To overcome this weakness, the parallel manipulator has found applications as the spindle or table of machine tools.[2-6] The accuracy is one of the primary needs of the precision machining. This needs a thorough understanding of the tool path programming.[7-9] The aim of this research is to partially meet this need and fill the gap in the literature in this respect.

Dasgupta and Mruthyunjaya[10] developed an algorithm for planning the singularity-free path of the Stewart mechanism. The algorithm limitations were its lack of confidence in detecting the non-existence of a singularity-free path and its sensitivity to intersections of singularity hypersurfaces. Shaw and Chen[11] investigated an algorithm for generating the cutting path of a Steward mechanism-based milling machine. Iso-scallop method and genetic algorithm are utilized respectively in the process for generating the cutting path and finding the singularity-free configurations of the tool in their research work. Merlet[12] presented trajectory evaluation for a classic Stewart mechanism. He developed a real-time method and errors have been controlled. Pugazhenthi et al.[13] developed an optimal algorithm for the trajectory planning of the hexapod machine tool in contour machining. In their study, a code has been developed to minimize the force requirement of the actuator and maximize the stiffness of the structure, and the constraints of workplace and singularity have been taken into account in their study. Peidong and Changlin[14] presented a novel approach to motion planning based on the planned trajectory on a parallel kinematic machine. Their approach was evaluated by the results of the simulation. Dash et al.[15] developed a numerical approach for path planning within the workspace borders of parallel mechanisms. Isolated singularities have been removed through routing method based on Grassmann's line geometry in their study. Afroun et al.[16,17] addressed an approach for generating an optimal motion for a DELTA parallel mechanism and Stewart platform manipulator. The sequential programming quadratic technique has been applied to find the spline control points' optimal position in their research. Harib et al.[18] presented an analytical method for trajectory planning of a redundant hybrid mechanism consisting of a Stewart Platform and a two

DOF (degree of freedom) rotary tilting table. Having presented eight coordinates, they defined five coordinates through conventional part programming and other three coordinates via trajectory planning. Li[19] considered tool path planning of hexapod parallel kinematic machines. In his study, appropriate trajectory planning is considered for nonlinear error reduction during the path. Jinsong[20] utilized kinematic nonlinearity of parallel machine tools to investigate their interpolation accuracy. Zheng[21] developed a path control algorithm for a parallel kinematic machine tool and applied it to the CNC system software. The developed algorithm has been verified by machining experiments. Chalak Qazani et al.[22-24] and Pedrammehr et al.[25,26] introduced hexarot mechanism as a novel six degree of freedom parallel manipulator and investigated its kinematics, dynamics and nonlinear error using image processing technique. The effective parameters on the nonlinear error of hexarot have also been determined in their study. They also studied the motion of machine tools' hexapod table on freeform surfaces with circular interpolation.[27]

In this study, by adding interpolation of various circular movements, movement capabilities of the interpolator unit are increased. Regarding the fact that in CNC machines, interpolation accuracy has a direct impact on accuracy; hence, in this study, an improved Tustin algorithm is used for interpolation of circular motion. Using image processing experimental tests, motion errors are obtained. Theoretical and experimental results are reasonably consistent with each other. In this study, two general cases are tested and the results of both cases are compared. In the first case, the nonlinear motion of table is ignored and interpolation is considered as a serial mechanism using both the theoretical and experimental methods. In the latter case, the nonlinear error interpolation of the platform is taken into account and also investigated via two theoretical and experimental methods. It should be noted that the algorithm developed for the circular interpolation is useful due to the low amount of nonlinear error. The physical specifications of the test manipulator are given in the Appendix.

2. Description of Hexapod Table

The mechanical prototype of a hexapod machine tool table developed for FP4M CNC machines and machining centers is shown in Fig. 1. It consists of a base fixed to the foundation, a moving platform accommodating the workpiece to be machined, and six identical pods the lower ends of which are connected to the base via universal joints and the upper ends are connected to the platform through spherical joints.

3. Motion Error of the Hexapod Table

In order to control error in an acceptable range, the value of nonlinear error must be obtained. Here in this research, Mid-oscillating circle is utilized to obtain the kinematic error (see Fig. 2).

Oscillating circle of a curve abuts the curve at a point. In other words, it has the same curvature and tangent as the curve has at that point. Just as the tangent line is the best line for approximating a curve at a given point, the osculating circle is the best circle which approximates the curve at a point. The osculating circle's radius is the inverse of curvature. This, however, is of critical importance both in the nonlinear motion of the table and its path programming.

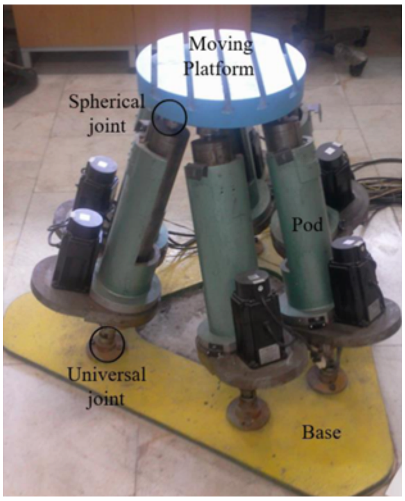

Fig. 1 The hexapod table

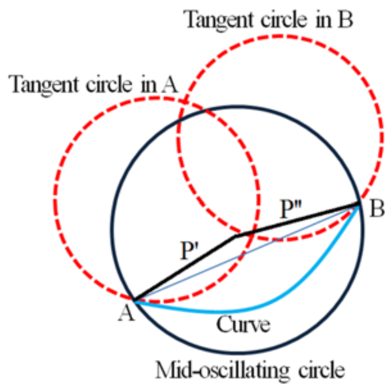

Fig. 2 Real and suitable paths

The vector normal to the plane consisting mid-oscillating circle, **h**, can be presented as follows:

$$\mathbf{h} = \mathbf{P} \times \mathbf{N} = \begin{bmatrix} i & j & k \\ P_x & P_y & P_z \\ N_x & N_y & N_z \end{bmatrix} \quad (1)$$

where **P** is the vector connecting two interpolated points A and B, and **N** is the unit vector normal to the tangent vector. **N** can be obtained as:

$$\mathbf{N} = \mathbf{a}/|\mathbf{a} \times \mathbf{v}| \quad (2)$$

In which **v** and **a** are the linear velocity and acceleration vectors of the platform between A and B, respectively.

Since points A and B are in the same plane and the vector **h** is its normal vector, the circular path's center can be calculated by solving the system of nonlinear equations as:

$$\begin{cases} (P'_x - C_x)^2 + (P'_y - C_y)^2 + (P'_z - C_z)^2 = \rho^2 \\ (P''_x - C_x)^2 + (P''_y - C_y)^2 + (P''_z - C_z)^2 = \rho^2 \\ h_x(C_x - P_x) + h_y(C_y - P_y) + h_z(C_z - P_z) = 0 \end{cases} \quad (3)$$

where $\mathbf{P}' = (P'_x, P'_y, P'_z)$ and $\mathbf{P}'' = (P''_x, P''_y, P''_z)$ are respectively position vectors of A and B points, and $\mathbf{C} = (C_x, C_y, C_z)$ is the mid-oscillating circle's center. The mid-oscillating circle's radius, ρ, can be determined as:

$$\rho = (\rho_A + \rho_B)/2 \tag{4}$$

where ρ_A and ρ_B are the osculating circle's radius at points A and B, respectively; ρ_A and ρ_B can be defined as:

$$\rho_A = 1/\kappa_A \tag{5}$$

$$\rho_B = 1/\kappa_B \tag{6}$$

In which κ_A and κ_B are curvatures in points A and B, respectively. Curvature can be calculated by the kinematics of pods and platform.[24,25]

Considering direct kinematic equations[24,25] and substituting Eq. (3) into Eqs. (5) and (6), kinematic error equation can be written as:

$$e = \rho - \sqrt{\rho^2 - (S/2)^2} \tag{7}$$

In Eq. (7), S is the curve's length between the A and B interpolated points (i.e. the proper path), and it can be obtained in terms of operator defined feedrate, F, and the time at which the control system responds to the servo motors, T_s, which yields:

$$S = FT_s \tag{8}$$

The maximum angular displacement between two interpolated points in terms of maximum nonlinear error, β, can be obtained as:

$$\beta = \mathrm{tg}^{-1}(e/2R) \tag{9}$$

where R (mm) is the radius of the interpolated circle.

Linear velocity and acceleration of the j^{th} pod in the i^{th} position, l'^{i}_{j} and l''^{i}_{j}, can be obtained solving the inverse kinematic problem of the mechanism,[28-32] which can be expressed as follows:

$$l'^{i}_{j} = (l^{i-1}_{j} - l^{i}_{j})/T_s \tag{10}$$

$$l''^{i}_{j} = (l'^{i-1}_{j} - l'^{i}_{j})/T_s \tag{11}$$

By having the length and linear velocities and accelerations of the pods, acceleration of the center of the moving platform can be calculated.[28] Substituting these data into Eqs. (2), (5) and (6) gives the curvature and the radius of oscillating-circle. If the kinematic error exceeds acceptable range, S has to be mitigated. In this condition, changing feed rate is of key importance in controlling the path length and kinematic error, and can be obtained using:

$$F = 2\sqrt{2\rho e_{all} - e_{all}^{2}}/T_s \tag{12}$$

where e_{all} is the maximum allowed error. The developed CNC code, in order to control error in the acceptable range, calculates the feed rate from Eq. (12) and replaces it with the previous one, and then begins other interpolation process based on the new feed rate.

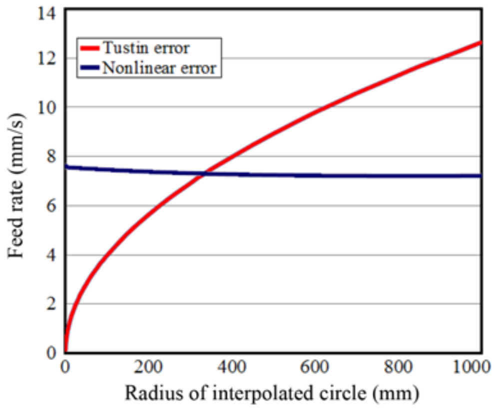

Fig. 3 Boundary conditions of 0.05 (mm) Tustin error and 0.25 (mm) nonlinear error

There are two main error sources in the circular interpolation of the hexapod table: one is a nonlinear error which is considered to be 0.25 (mm) at maximum and other is Tustin error with 0.05 (mm) maximum allowance. These allowances, however, are assumed considering the accuracy of the utilized measurement system (i.e., image processing).

Considering improved Tustin algorithm, the maximum angular displacement between two interpolated points, α, can be obtained as:

$$\alpha = \sqrt{16/(R-1)} = 4/\sqrt{R} \tag{13}$$

In Eq. (13), R is the radius of the interpolated circle and it is in Basic Length Unit (BLU) terms.

Considering T_s=0.1 (s), Eq. (12) can be rewritten compactly as:

$$F = 4\sqrt{R}/T_s \tag{14}$$

Solving direct kinematic relations,[27] the feed rate of the table with a maximum error range of 0.25 can be obtained. Tustin error can also be obtained via Eq. (14). The results for both errors are illustrated in Fig. 3 for different radiuses of interpolated circles and feed rates.

The intersection point of two nonlinear error and Tustin error curves in Fig. 3 gives the radius which is consist of the maximum feed rate of the table with minimum error.

4. Circular Interpolation Algorithm

Tool path programing for machine tools' hexapod table is developed based on circular interpolation. The main purpose of this research is to add different kinds of circular interpolators to the hexapod interpolator unit, to enable the table to have circular motions in a clockwise direction and vice versa within its workspace. The nonlinear error is also investigated to improve the accuracy of the circular interpolation.

There are two standards for using G-code in a circular motion: one is using I and J parameters which define the geometry center of the moving platform according to its initial point, the other method is utilizing Circle Radius (CR) parameter which specifies the radius of the

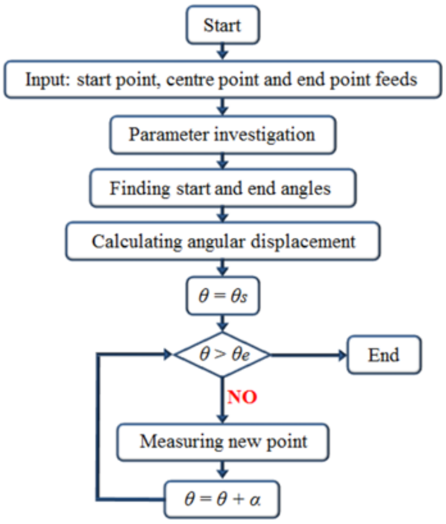

Fig. 4 Clockwise circular motion algorithm of the hexapod table

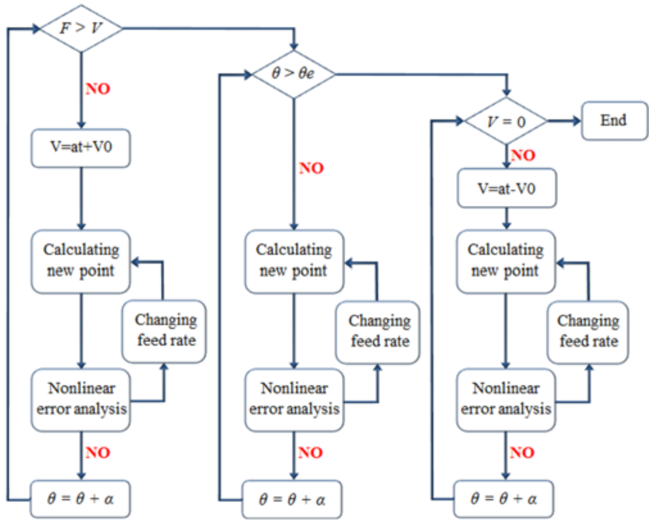

Fig. 5 Details for the interpolation step of the algorithm

circle.[33] In the second method, if CR is positive, the angular motion of the circle will be lower than 180 degrees, and vice versa. Fig. 4 presents the developed algorithm for the clockwise circular motion of the hexapod table.

The first step in Fig. 4 includes: start point of circular motion which is determined by existed position of the tool, the end point of circular motion which is determined by defined parameters in the same command and circle center which is determined after primary calculations and independent from determining method. Using these parameters the circle is determined and an interpolation is performed.

The second step is to verify input data. Since the operator may make a mistake in setting the parameters associated with the circle, the program is able to check the parameters in this step. If the parameters associated with the circle are not verified, a message will be sent to the operator to check and modify the parameters. First, circles radius is obtained for the start and end points of circular motion. By comparing the two numbers, if their absolute difference is greater than 0.05 (mm), the error message will appear. Consideration of 0.05 (mm) difference between these two numbers is due to the numerical solution which is carried out by the algorithm.

The third step is associated with start and end angles of the circle. To perform more speedy interpolation and to reduce the amount of computation, machine's center point is transferred to the circle center using a matrix. Considering four areas of the trigonometric circle, the start and end angles of the circle, i.e., θ, are calculated as follows:

$$\theta = tg^{-1}(J/I)\ :\ \begin{cases} if\ 0 \le \theta < \pi/2 \Rightarrow \theta = \theta \\ if\ \pi/2 \le \theta < 3\pi/2 \Rightarrow \theta = \theta + \pi \\ if\ 3\pi/2 \le \theta < 2\pi \Rightarrow \theta = \theta + 2\pi \end{cases} \tag{15}$$

The fourth step calculates β and α from Eqs. (9) and (13), respectively. The fifth step in Fig. 4, $\theta = \theta_s$, indicates the interpolation step of the algorithm. The details of this step, moreover, are presented in Fig. 5. In this step, considering the predefined acceleration (50 mm/s^2, in this study), the accelerator unit of the table correlates the velocity of the table to the velocity defined by operator, then platform moves with constant velocity, and finally the accelerator unit of the table acts to reduce the velocity of the moving platform. Nonlinear error analysis is performed for all the steps of the trapezoidal velocity profile. Feed rate is changed by Eq. (11) to obtain a proper S and control kinematic error.

5. Experimental Test

Image processing is one of the available methods for measuring the movement of the various dynamic systems. In this method, using a camcorder, determined positions of target motion on the platform is filmed. Recorded videos are imported to software which is designed to image processing. First, this software divides the video into the constituent frames and provides a matrix for each frame. Elements of this matrix are a number of pixels in each frame. For each matrix element, numbers between 0 and 256 are selected by the software. For example, white and complete black have numbers 0 and 256, respectively. Target coordinate is imported to the software by the photo which is taken from the first frame of the original film. So, the application finds the status of this small matrix in the larger matrix and it follows the motion in next frames. Thus, at the end of the movement, motion coordinate is obtained in pixels. Finally, regarding the relationship between the number of pixels and targets diameters, using a coefficient, equation of motion is obtained (Fig. 6).

For the test, two camcorders are used in two directions in order to film the target motion (Fig. 7). After filming starts, run command of the machine is provided so that the hexapod table and target on it, starts to move. Cameras number 1 and 2 record movements in YZ and XZ planes, respectively. In order to make the camera lens perpendicular to the spherical target, camera base is completely aligned with ground level. To adjust the lens in the direction of the coordinate axes in the XY plane, table target is moved in x and y directions and the distance between camera and target is measured. This distance is kept fixed in a perpendicular direction with rotating the camera and moving the hexapod table. It should be noted that this process is performed for both cameras. The specification of the employed sensor for the experimental

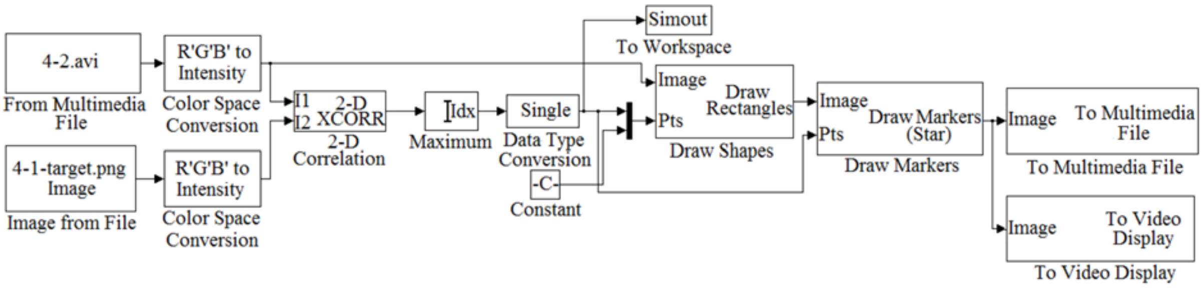

Fig. 6 Block diagram of image processing

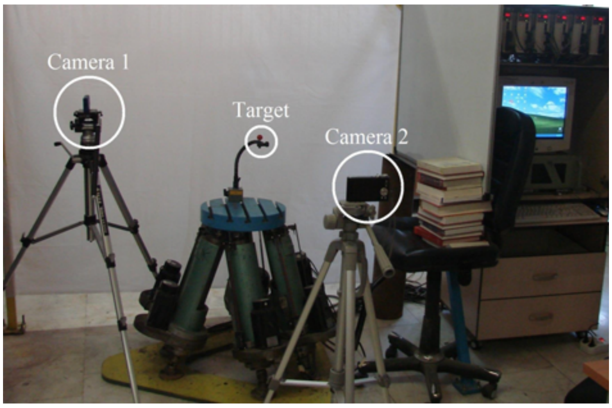

Fig. 7 Image processing setup

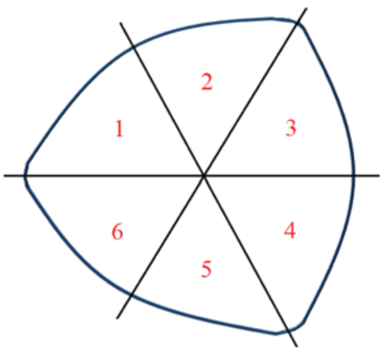

Fig. 8 Cross section of workspace for the hexapod in Z=750 (mm)

testing is given in the Appendix.

In this paper, two general conditions have been experimentally tested and results have been compared with each other. In the first case, the nonlinear motion of the table is neglected and interpolation is carried out as a serial mechanism with both simulation and experimental methods. In the latter case, the nonlinear error interpolation of the platform is taken into account and controlled. Due to a decrease in nonlinear error in the second case, it can be concluded that the program used for hexapod to carry out the circular motion is quite convenient.

Since the nonlinear error rate differs in various areas of the workspace, the workspace of the mechanism is of utmost importance in determining and controlling this error. Assuming a cross section of the workspace in the Z direction, and regarding the origin of coordinates which is at the center of the table, three symmetrical planes with six areas can be considered within the workspace of the table (Fig. 8).

Table 1 Various parameters considered as Taguchi levels and classes

Classes (Taguchi, L32)	Workspace (mm)	Feed rate (mm/s)	Radius (mm)
Level one	area 1 to 3, z=650	5	300
Level two	area 1 to 4, z=650	10	500
Level three	area 1 to 3, z=750	20	700
Level four	area 1 to 4, z=750	25	1000

Considering three symmetrical planes shown in Fig. 8, all circular motions within the workspace and with the specified height can be provided with three circular motions. In this study, due to the similarity of motions, circular motions in two surrounding environments are neglected. In the first motion, start point and end point of the motion in the workspace lies in areas 1 and 3, respectively. This motion is the same as movements from areas 1 to 5, 2 to 4, 2 to 6 and 3 to 5. In the second one, start point and end point of the motion in the workspace lies in areas 1 and 4 respectively. This motion is similar to movements from areas 2 to 5 and 3 to 6.

One of the effective parameters is the height of the workspace. The lower the height, the larger the curvature of the curve will be. In this paper, the parameter Z is examined in two cases of 650 (mm) and 750 (mm).

Feed rate is the other parameter which affects the error rate. In a way that by increasing the amount of feed rate, the number of resulted points from interpolation will decrease and consequently point distance and error will increase. Regarding hexapod control system and its servo motors, four different feed rates of 5, 10, 20 and 25 (mm/s) have been selected and investigated in this paper.

Another parameter affecting the error is the radius of the interpolated circle. Regarding the nonlinear and Tustin errors, there is an optimal radius that provides access to least error with most feed rate. In this research, Tustin and nonlinear motion errors are considered 0.25 (mm) and 0.05 (mm), respectively, so the optimal radius has a value between 650 (mm) to 700 (mm) of interpolation circle radius.

The test has three effective factors including workspace, feed rate and radius of the interpolated circle. Each of these factors is considered as classes of Taguchi method and each class has 4 levels (Table 1). Thus, full factorial of test equals to 64 in which by using Taguchi method it is possible to reduce the test numbers to 16. In this paper, considering the proportion of feed rate parameter and output of the workforce, L32 method is used.[34]

After considering corresponding outputs of each camcorder, the

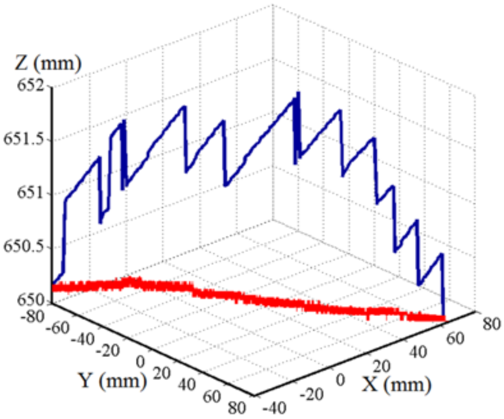

Fig. 9 The motion diagram of the platform center regardless of its nonlinear motion, R=1000 (mm), F=5 (mm/s), moving from area 1 to 3 and Z=650 (mm)

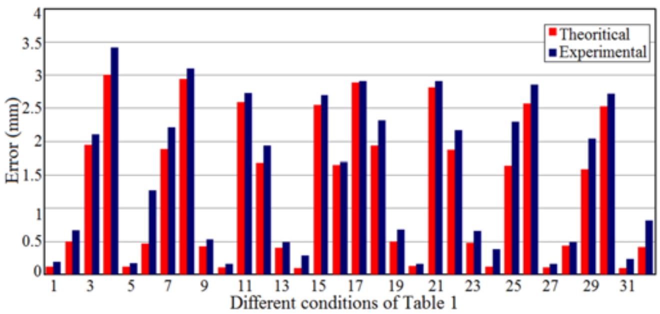

Fig. 10 Comparison of experimental and theoretical results by neglecting the nonlinear motion of the table

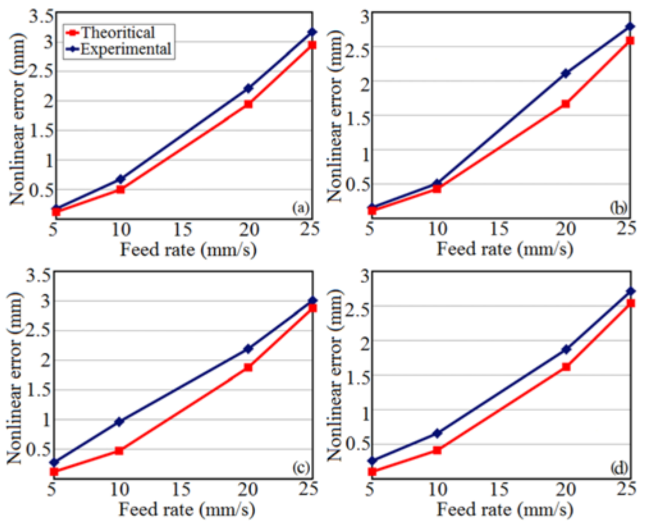

Fig. 11 Effects of feed rate changes on error in circular motion by neglecting the nonlinear motion of the table: (a) motion from areas 1 to 3, Z=650 (mm) (b) motion from areas 1 to 3, Z=750 (mm) (c) motion from areas 1 to 4, Z=650 (mm) (d) motion from areas 1 to 4, Z=750 (mm)

motion diagram of the platform center will be obtained (Fig. 9).

Having this motion diagram at hand, the nonlinear error can be

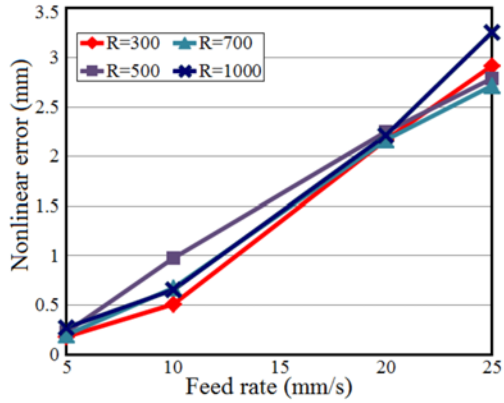

Fig. 12 Effects of feed rate changes on an error in specified radius and in a circular motion by neglecting the nonlinear motion of the table

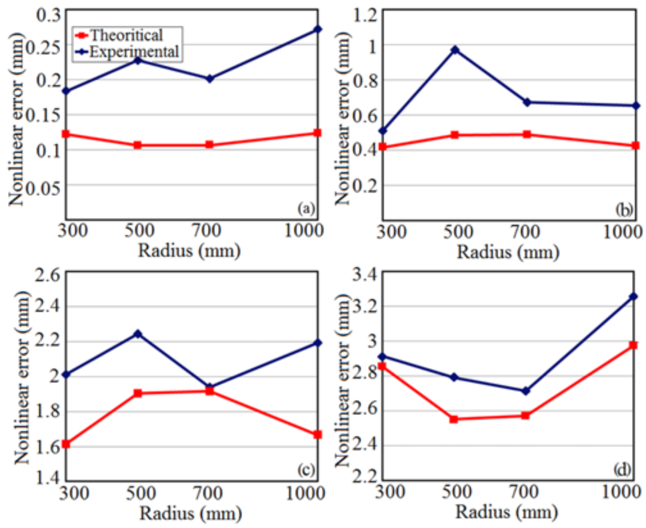

Fig. 13 Effects of the changes of interpolated circle radius on error in different feed rates and by neglecting the nonlinear motion of the table: (a) F=5 (mm/s) (b) F=10 (mm/s) (c) F=20 (mm/s) (d) F=25 (mm/s)

calculated using a mid-oscillating circle. In Fig. 9 the distance from the platform center to the circle obtained from the projection of its motion diagram on plane Z=650 provides the nonlinear error in experimental testing.

6. Results and Discussions

Neglecting the nonlinear motion of the platform, Fig. 10 illustrates table's motion error both theoretically and experimentally. Since the error rate in this condition lies in the calculation range of the measurement system, the difference between the results obtained from the experimental test and theoretical method is so low. This, however, shows the accuracy of the results.

Fig. 11 presents the effects of feed rate changes on error regardless of table's nonlinear motion. Regarding Figs. 11(a) and 11(b) or Figs.

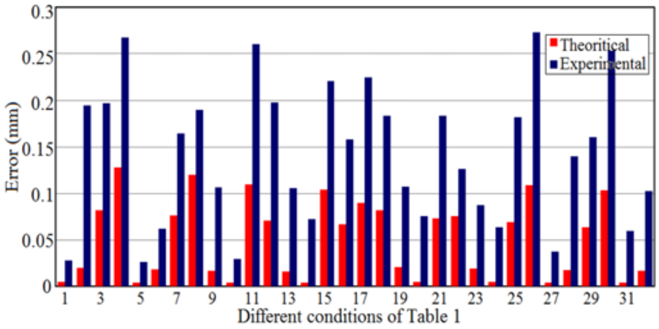

Fig. 14 Comparison of experimental and theoretical results taking into account the nonlinear motion of the table

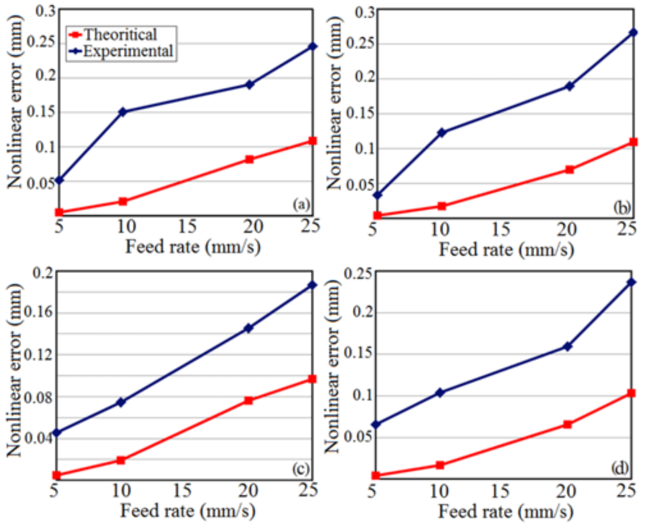

Fig. 15 Effects of feed rate changes on error in circular motion considering the nonlinear motion of the table: (a) motion from areas 1 to 3, Z=650 (mm) (b) motion from areas 1 to 3, Z=750 (mm) (c) motion from areas 1 to 4, Z=650 (mm) (d) motion from areas 1 to 4, Z=750 (mm)

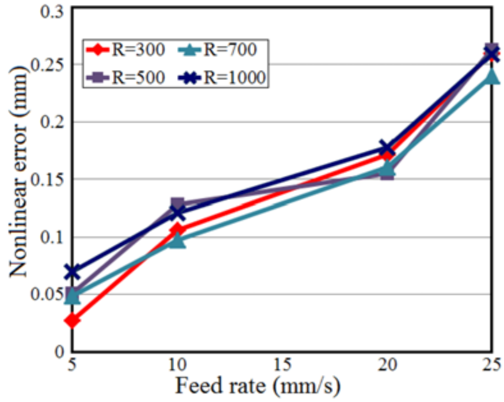

Fig. 16 Effects of feed rate changes on the error in specified radius and in circular motion considering the nonlinear motion of the table

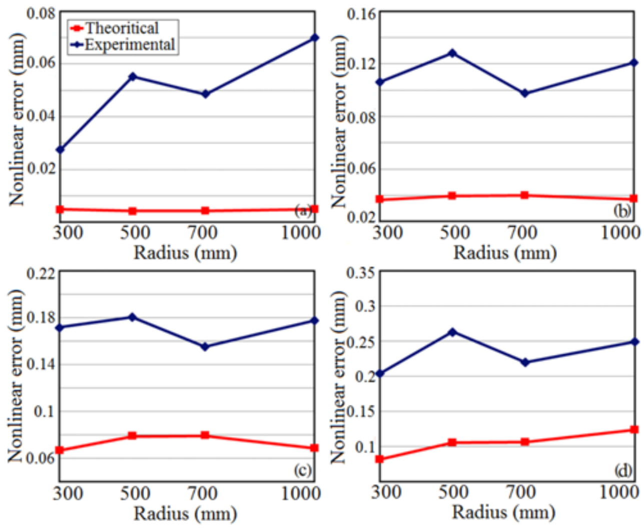

Fig. 17 Effects of the changes of interpolated circle radius on error in different feed rates and considering the nonlinear motion of the table: (a) F=5 (mm/s) (b) F=10 (mm/s) (c) F=20 (mm/s) (d) F=25 (mm/s)

11(c) and 11(d), it should be noted that error rate decreases by an increase in Z. This, however, is because of the high amount of curvature in the low height of workspace of the table. Also by comparing Figs. 11(a) and 11(c) or Figs. 11(b) and 11(d), it is obvious that the error rate in the movement from areas 1 to 3 is larger to that of table movement from areas 1 to 4. Therefore, it could be estimated that the curvature is larger in the movement from areas 1 to 3.

Fig. 12 presents the effects of feed rate changes on the error in specified radiuses, by neglecting the nonlinear motion of the table. Regarding Fig. 12, it is quite apparent that radius of 700 (mm) provides the most amount of feed rate with a least possible error.

Fig. 13 shows how the error changes occur regarding the radius changes where the nonlinear motion of table is neglected. As it is clearly seen in this figure, an increase of feed rate leads to increase of error. Also, interpolated circle with a radius of 700 (mm) has the least error rate in different feed rates.

By considering the nonlinear motion of the table, Fig. 14 illustrates table motion errors both theoretically and experimentally. In this bar chart difference between the results obtained from theoretical and image processing is approximately perceptible. This, however, is due to the lack of conformity of measurement system accuracy within the error range. However, similar trends are clearly evident in both cases.

By taking the nonlinear motion of the table into the account, Fig. 15 shows the effects of feed rate changes on error. Comparing Fig. 15 with Fig. 11 makes it evident that error increase rate reduces by an increase in feed rate where the table's nonlinear motion is taken into consideration. This is due to the capability of interpolation algorithm which checks error rate for each step and acts to reduce it.

By taking into the account the nonlinear motion of the table, Fig. 16 illustrates the effects of feed rate changes on the error in specified radiuses. Regarding both Figs. 12 and 16, it is completely clear that radius of 700 (mm) is the most suitable radius for interpolation which provides the most amount of feed rate with a least possible error.

How the error changes occur regarding the radius changes is also presented in Fig. 17. As Fig. 15, it is seen in this figure the increase of feed rate results in error increase. Also interpolated circle with a radius of 700 (mm) has the least error rate in various feed rates.

7. Conclusions

In this paper, a comprehensive algorithm for the tool path programming of the hexapod table is developed. This algorithm is developed based on a circular motion using C#.Net which has the capability of checking nonlinear motion error and keep it in a controlled range. In the circular motion of the table, the optimal radius which provides access to maximum feed rate and least error is obtained by solving Tustin and nonlinear error equations. It can be concluded that the error increases with increasing the feed rate, and nonlinear error for circular motion in low heights is more than that of higher heights. Furthermore, using the algorithm presented in this paper, error increase rate can be reduced when the feed rate is increased.

REFERENCES

1. Zhang, D., “Parallel Robotic Machine Tools,” Springer Science & Business Media, 2009.
2. Chi, Z., Zhang, D., Xia, L., and Gao, Z., “Multi-Objective Optimization of Stiffness and Workspace for a Parallel Kinematic Machine,” International Journal of Mechanics and Materials in Design, Vol. 9, No. 3, pp. 281-293, 2013.
3. Pedrammehr, S., Mahboubkhah, M., and Khani, N., “A Study on Vibration of Stewart Platform-Based Machine Tool Table,” The International Journal of Advanced Manufacturing Technology, Vol. 65, Nos. 5-8, pp. 991-1007, 2013.
4. Pedrammehr, S., Mahboubkhah, M., Qazani, M. R. C., Rahmani, A., and Pakzad, S., “Forced Vibration Analysis of Milling Machine’s Hexapod Table under Machining Forces,” Strojniški vestnik-Journal of Mechanical Engineering, Vol. 60, No. 3, pp. 158-171, 2014.
5. Pedrammehr, S., Mahboubkhah, M., and Khani, N., “Natural Frequencies and Mode Shapes for Vibrations of Machine Tools’ Hexapod Table,” Proc. of 1st International Conference on Acoustics and Vibration ISAV 2011, pp. 21-22, 2011.
6. Pedrammehr, S., “Investigation of Factors Influential on the Dynamic Features of Machine Tools’ Hexapod Table,” Proc. of 2nd International Conference on Acoustics and Vibration, 2012.
7. Gao, Z. and Zhang, D., “Simulation Driven Performance Characterization of a Spatial Compliant Parallel Mechanism,” International Journal of Mechanics and Materials in Design, Vol. 10, No. 3, pp. 227-246, 2014.
8. Jia, Z.-Y., Lin, S., and Liu, W., “Measurement Method of Six-Axis Load Sharing Based on the Stewart Platform,” Measurement, Vol. 43, No. 3, pp. 329-335, 2010.
9. Rahmani, A., Ghanbari, A., and Pedrammehr, S., “Kinematic Analysis for Hybrid 2-(6-UPU) Manipulator by Wavelet Neural Network,” Advanced Materials Research, Vol. 1016, pp. 726-730, 2014.
10. Dasgupta, B. and Mruthyunjaya, T., “Singularity-Free Path Planning for the Stewart Platform Manipulator,” Mechanism and Machine Theory, Vol. 33, No. 6, pp. 711-725, 1998.
11. Shaw, D. and Chen, Y.-S., “Cutting Path Generation of the Stewart-Platform-Based Milling Machine Using an End-Mill,” International Journal of Production Research, Vol. 39, No. 7, pp. 1367-1383, 2001.
12. Merlet, J.-P., “A Generic Trajectory Verifier for the Motion Planning of Parallel Robots,” Journal of Mechanical Design, Vol. 123, No. 4, pp. 510-515, 2001.
13. Pugazhenthi, S., Nagarajan, T., and Singaperumal, M., “Optimal Trajectory Planning for a Hexapod Machine Tool during Contour Machining,” Proceedings of the Institution of Mechanical Engineers, Part C: Journal of Mechanical Engineering Science, Vol. 216, No. 12, pp. 1247-1257, 2002.
14. Wu, P. and Wu, C., “Motion Planning and Coupling Analysis Based on 3-RRR (4r) Parallel Mechanism,” International Journal of Mechanics and Materials in Design, Vol. 4, No. 3, pp. 325-331, 2008.
15. Dash, A. K., Chen, I.-M., Yeo, S.H., and Yang, G., “Workspace Generation and Planning Singularity-Free Path for Parallel Manipulators,” Mechanism and Machine Theory, Vol. 40, No. 7, pp. 776-805, 2005.
16. Afroun, M., Chettibi, T., and Hanchi, S., “Planning Optimal Motions for a Delta Parallel Robot,” Proc. of 14th Mediterranean Conference on Control and Automation, pp. 1-6, 2006.
17. Afroun, M., Chettibi, T., Hanchi, S., Dequidt, A., and Vermeiren, L., “Optimal Motions Planning for a Gough Parallel Robot,” Proc. of 16th Mediterranean Conference on Control and Automation, pp. 493-498, 2008.
18. Harib, K., Ullah, A. S., and Hammami, A., “A Hexapod-Based Machine Tool with Hybrid Structure: Kinematic Analysis and Trajectory Planning,” International Journal of Machine Tools and Manufacture, Vol. 47, No. 9, pp. 1426-1432, 2007.
19. Li, Z., “Reconfiguration and Tool Path Planning of Hexapod Machine Tools,” Ph.D. Thesis, New Jersey Institute of Technology, 2000.
20. Wang, J., Wang, Z., Huang, T., and Whitehouse, D., “Nonlinearity for a Parallel Kinematic Machine Tool and Its Application to Interpolation Accuracy Analysis,” Science in China Series E: Technological Sciences, Vol. 45, No. 1, pp. 97-105, 2002.
21. Zheng, K.-J., Gao, J.-S., and Zhao, Y.-S., “Path Control Algorithms of a Novel 5-DOF Parallel Machine Tool,” Proc. of IEEE International Conference on Mechatronics and Automation, pp. 1381-1385, 2005.
22. Pedrammehr, S., Qazani, M. R. C., Abdi, H., and Nahavandi, S., “Mathematical Modelling of Linear Motion Error for Hexarot

Parallel Manipulators," Applied Mathematical Modelling, Vol. 40, No. 2, pp. 942-954, 2016.

23. Pedrammehr, S., Nahavandi, S., and Abdi, H., "Closed-Form Dynamics of Hexarot Parallel Manipulator by Means of the Principle of Virtual Work," Acta Mechanica Sinica, 2018. (DOI: 10.1007/s10409-018-0761-4)

24. Pedrammehr, S., Nahavandi, S., and Abdi, H., "Evaluation of Inverse Dynamics of Hexarot-based Centrifugal Simulators," International Journal of Dynamics and Control, pp. 1-11, 2018. (DOI: 10.1007/s40435-018-0421-3)

25. Pedrammehr, S., Danaei, B., Abdi, H., Masouleh, M. T., and Nahavandi, S., "Dynamic Analysis of Hexarot: Axis-Symmetric Parallel Manipulator," Robotica, Vol. 36, No. 2, pp. 225-240, 2018.

26. Pedrammehr, S., Najdovski, Z., Abdi, H., and Nahavandi, S., "Design Methodology for a Hexarot-Based Centrifugal High-G Simulator," IEEE International Conference on Systems, Man, and Cybernetics, IEEE SMC 2017, 2017.

27. Qazani, M. R. C., Pedrammehr, S., and Nategh, M. J., "A Study on Motion of Machine Tools' Hexapod Table on Freeform Surfaces with Circular Interpolation," The International Journal of Advanced Manufacturing Technology, Vol. 75, Nos. 9-12, pp. 1763-1771, 2014.

28. Heisel, U. and Gringel, M., "Machine Tool Design Requirements for High-Speed Machining," CIRP Annals-Manufacturing Technology, Vol. 45, No. 1, pp. 389-392, 1996.

29. Harib, K. and Srinivasan, K., "Kinematic and Dynamic Analysis of Stewart Platform-Based Machine Tool Structures," Robotica, Vol. 21, No. 5, pp. 541-554, 2003.

30. Li, Y.-J., Wang, G.-C., Zhang, J., and Jia, Z.-Y., "Dynamic Characteristics of Piezoelectric Six-Dimensional Heavy Force/Moment Sensor for Large-Load Robotic Manipulator," Measurement, Vol. 45, No. 5, pp. 1114-1125, 2012.

31. Pedrammehr, S., Mahboubkhah, M., and Pakzad, S., "An Improved Solution to the Inverse Dynamics of the General Stewart Platform," Proc. of IEEE International Conference on Mechatronics (ICM), pp. 392-397, 2011.

32. Pedrammehr, S., Mahboubkhah, M., and Khani, N., "Improved Dynamic Equations for the Generally Configured Stewart Platform Manipulator," Journal of Mechanical Science and Technology, Vol. 26, No. 3, pp. 711-721, 2012.

33. Nanfara, F., Uccello, T., and Murphy, D., "The CNC Workbook," An Introduction to Computer Numerical Control, 1995.

34. Roy, R. K., "Design of Experiments Using the Taguchi Approach: 16 Steps to Product and Process Improvement," John Wiley & Sons, 2001.

APPENDIX

Sensor specification is as the following:
Brand: Canon;
Model: IXY DIGITAL 920 IS;
Megapixels: 10.00;
Sensor resolution: 3647 × 2742
ACCU: This is the actual size of the **IXY DIGITAL 920 IS** sensor: 1/2.3" ~ 6.16 × 4.62 (mm)

The physical specifications of the test manipulator are as follows:
Radius of the moving platform = 175 (mm);
Radius of the base = 400 (mm);
Angular distance between two adjacent spherical joints = 30°;
Angular distance between two adjacent universal joints = 14°;
Minimum Length of each pod = 760.2 (mm);
Maximum Length of each pod = 968.9 (mm);
Maximum course in X axis = ±130 (mm), in Y axis = ±130 (mm), and in Z axis = 220 (mm);
The precision of the manipulator = 0.05 (mm).